J Sol-Gel Sci Technol (2014) 71:458–463
DOI 10.1007/s10971-014-3400-y

ORIGINAL PAPER

High-k titanium–aluminum oxide dielectric films prepared by inorganic–organic hybrid solution

Juan Peng · Chenhang Sheng · Jifeng Shi · Xifeng Li · Jianhua Zhang

Received: 10 February 2014 / Accepted: 10 May 2014 / Published online: 21 May 2014

Abstract In this paper, high-k titanium–aluminum oxide (ATO) dielectric film has been realized by using organic–inorganic hybrid precursor solution. X-ray diffraction pattern revealed that the ATO films (Ti content less than 67 at%) remain amorphous phase for annealing treatment at 400 °C. And all of the amorphous ATO films had very smooth and uniform surface with root mean square (RMS) roughness of less than 0.5 nm. Meanwhile, the results showed that the ATO film (Ti:Al = 1:8) had the best performance, including RMS roughness of 0.33 nm, relative permittivity of 15, and leakage current density of 1.41×10^{-6} A/cm^2 at 1 MV/cm.

Keywords Titanium–aluminum oxide (ATO) · Solution process · Amorphous · Relative permittivity · Leakage current density

1 Introduction

The rapid constriction of the transistor feature size had forced the gate dielectric thickness to decrease rapidly [1]. Therefore, alternative dielectrics with substantially higher dielectric constant attracted much attention. Meanwhile, transistor gate dielectric layer should have very smooth surface, free from charge-trapping defects, and exhibit low-leakage current under applied voltages [2]. To realize those demands, high-k materials, such as TiO_2, Y_2O_3 [3], Gd_2O_3 [4], ZrO_2 [5], HfO_2 [6], Ta_2O_5 [7], and Al_2O_3 [8, 9], are being considered for their unique advantages such as high capacitance with low leakage current, and good thermodynamic stability. Among those high-k materials, Al_2O_3 exhibits the largest band gap of 8.9 eV and a relative permittivity of 9, and Al_2O_3 is thermodynamically stable and low interfacial trap density with oxide semiconductors [9–11]. TiO_2 is another well known high-k dielectric due to its extraordinarily high dielectric constant which more than 50 [1]. However, TiO_2 has large leakage current owing to its low crystallization temperature of 150 °C [12] and narrow band gap of 3.0–3.2 eV [10]. Fortunately, electrically unstable TiO_2 films is expected to be tailored to be a good current control layer by the insertion of insulating Al_2O_3 interlayer [13], TiO_2–Al_2O_3 (ATO) dielectric film has been made in many ways, such as cyclic chemical vapor deposition (CVD) [14], atomic layer deposition (ALD) [13, 15], sputtering [16], plasma-enhanced chemical vapor deposition (PECVD) [17], and solution [10]. Solution-based coating methods have many advantages, such as simplicity, low cost, high throughput and controllable component.

However, solution-processed ATO films were prepared by using expensively organic precursor [10], and the preparation process was rather complex, which restricts low cost and large area fabrication. It is worth studying ATO films fabricated from inorganic precursor. In this paper, the ATO films were developed with an organic–inorganic hybrid precursor solution which is a viable alternative to organic solution due to its simplicity and low processing cost. Besides, this hybrid solution has its unique characteristics of components molecularly dispersed in the sol stage, with the hybrid films inner component achieving nanometer level. The surface morphology, optical, and

J. Peng · C. Sheng · J. Shi · X. Li (✉) · J. Zhang (✉)
Key Laboratory of Advanced Display and System Application, Ministry of Education, Shanghai University, Shanghai 200072, China
e-mail: lixifeng@shu.edu.cn

J. Zhang
e-mail: jhzhang@shu.edu.cn

electrical properties of the ATO films were investigated in details.

2 Experimental

The 0.3 M precursor solution of ATO was prepared by dissolving titanium tetrachloride in 2-methoxyethanol (2-MOE), after stirring for half an hour, small amount of deionized water was added and then mixed with aluminum tri-*sec*-butoxide in titanium solution. After that a 0.3 M monoethanolamine (MEA) was added in the precursor solution as a stabilizer. The mole ratio of Ti and Al varies from 1:0 to 0:1 (1:0, 8:1, 2:1, 1:1, 1:2, 1:8, and 0:1, and the corresponding Ti content was 100, 87, 67, 50, 33, 13, and 0 at%, respectively). After thoroughly mixing, the solution was stirred at 70 °C for 3 h and then aged for 24 h.

A thin film of the precursor solution was deposited by spin-coating at 3,000 rpm for 30 s, and heating at 160 °C for 15 min to remove solvent after each coating. The same procedure was repeated several times in order to get a suitable thickness. Post-annealing was performed at 400 °C for 2 h to remove the residual chemicals and improve the performance of the ATO film.

For metal–insulator–metal (MIM) capacitor structure (Al/ATO/ITO/glass), which to analyze the relative dielectric constant (ε_r), the indium tin oxide (ITO) layer was deposited on the Corning EXG glass with the size of 200 × 200 mm by sputter-deposition process, firstly. Then the ATO film was deposited on the ITO/glass substrate as described above. Lastly, the upper electrodes—dot-patterned Al layer was deposited by evaporated on the ATO/ITO/glass substrate using a shadow mask.

The cross-section morphology of MIM structure was observed by scanning electron microscope (SEM, S-4800, Hatachi). The ATO structural information was obtained using X-ray diffraction (XRD, DLMAX-2200, Rigaku). The surface roughness of the ATO was investigated by atomic force microscope (AFM, SPI 4000, SII Nano Technology). The ultraviolet/visible (UV/VIS) optical transmission spectrum of the ATO thin films on the quartz substrate was characterized using a UV/VIS spectrophotometer (Hatachi,S-3900). Capacitance (C)–voltage (V) characteristics were determined using an Agilent E4980A precision LCR meter, and current (I)–voltage (V) characteristics were determined using an Agilent 5155C semiconductor parameter analyzer.

3 Result and discussion

Figure 1 shows the XRD patterns of ATO films annealed at 400 °C with different mixing components. No diffraction peaks can be detected from XRD patterns of the films

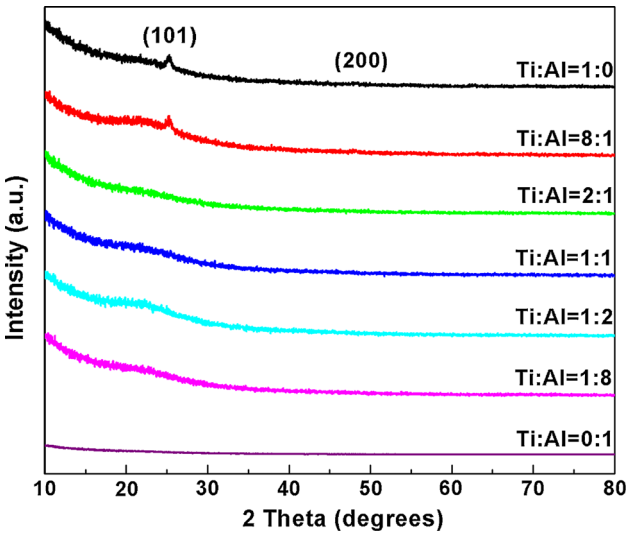

Fig. 1 XRD patterns of ATO films with various Ti content

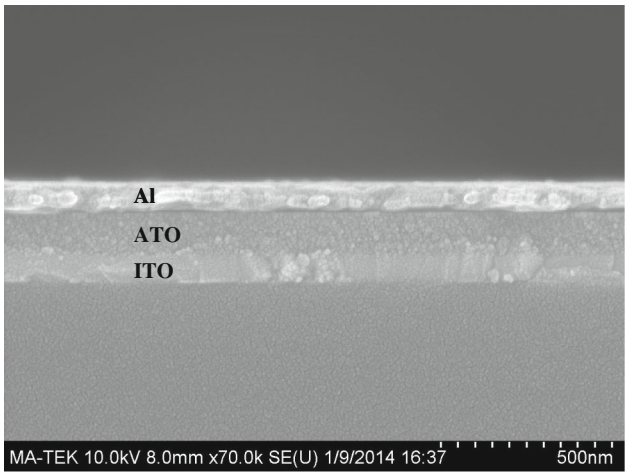

Fig. 2 Cross-sectional SEM image of typical ATO film

(Ti < 67 at%), indicating an amorphous phase. With the increasing of Ti amount (Ti > 67 at%) further, an abrupt peak (at 25.3°) and a weak peak (at 48.3°) were observed, indicating polycrystalline phase, which are characteristic of the (101) and (200) orientations of anatase TiO_2 [17, 18]. The result clearly revealed that the crystallize temperature of ATO films was highly dependent on the concentration of Ti, which is consistent with the literature reported [19].

Figure 2 shows the SEM cross-section morphology of Al_2O_3/ATO/ITO/glass structure. It was shown that the thickness of the typical ATO films is about 140 nm, and the ATO films were dense and free of pore. Surface morphologies of the ATO films are illustrated in Fig. 3(a)–(g). The surfaces of (a)–(e) films appears quite smooth, uniform and pinhole-free, which may be prone to the decrease of leakage current density as dielectric layer. Figure 4 illustrates the dependence of the RMS roughness and peak–

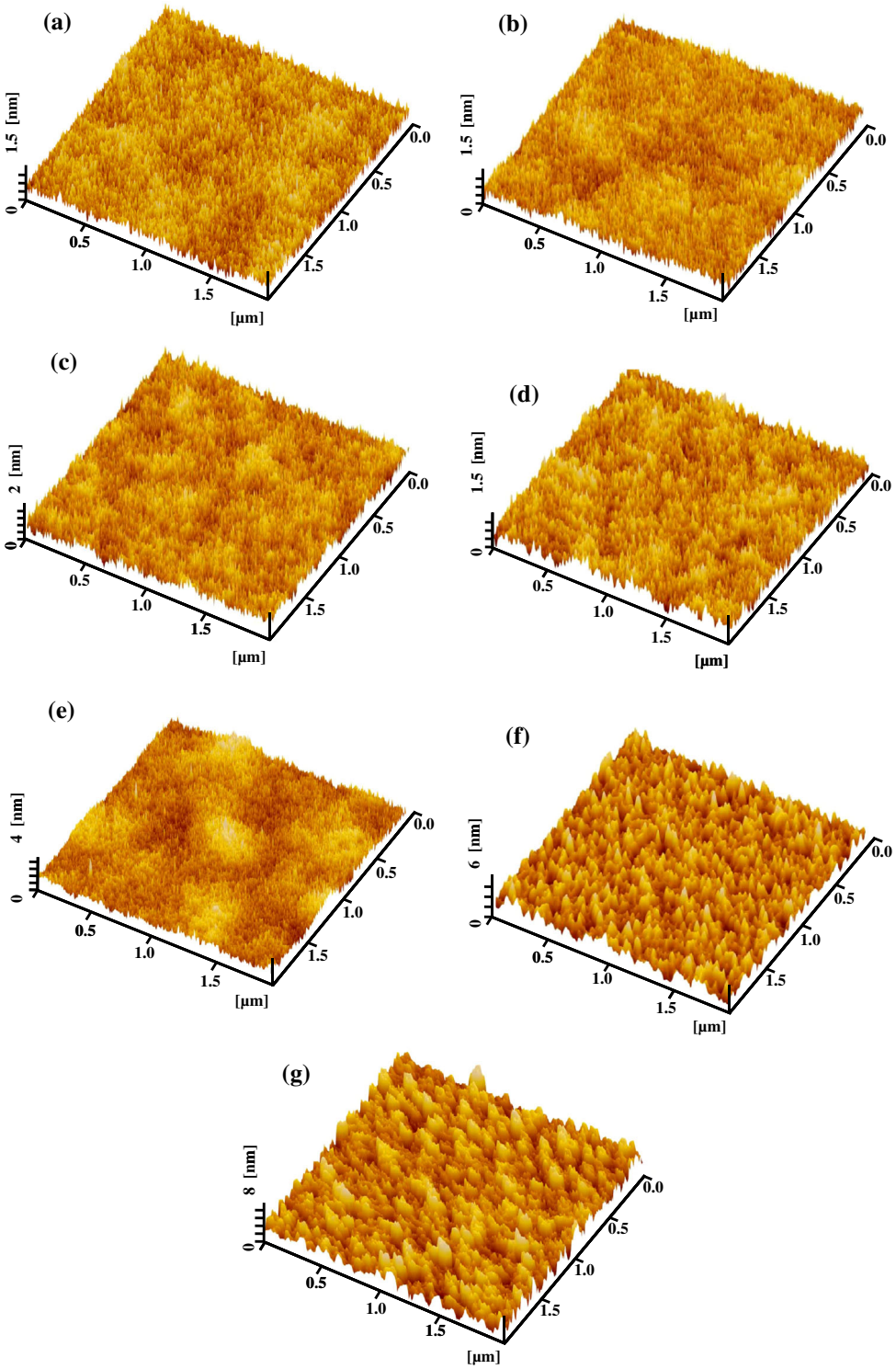

Fig. 3 AFM images of surface morphology of ATO films with different ratio of Ti and Al: **a** 0:1, **b** 1:8, **c** 1:2, **d** 1:1, **e** 2:1, **f** 8:1, and **g** 1:0

valley roughness (R_{P-V}) on the concentration of Ti. The RMS roughness of the ATO films increases as the concentration of Ti increases monotonically, the ATO film (Ti:Al = 1:0) has the biggest roughness of 1.21 nm due to the polycrystalline nature of the titanium oxide, which is consistent with the previously report well [17]. The R_{P-V} had no evidently change as Ti content was less than 50 at%, and then rise quickly when Ti content increases continually, which is due to crystallization of ATO films as confirmed by XRD results. The high R_{P-V} maybe results in a high electric field and breakdown of films, leading to exponentially increasing of leakage current [20].

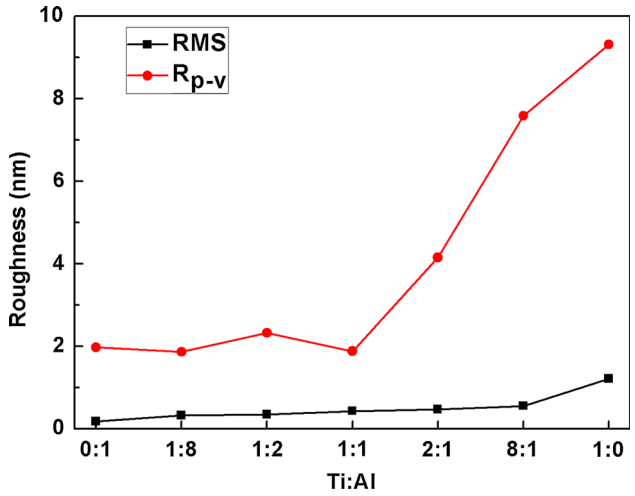

Fig. 4 Roughness of ATO films as a function of Ti content

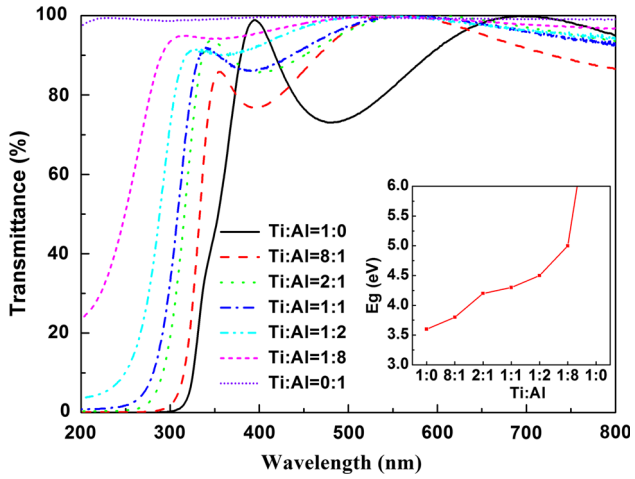

Fig. 5 Transmittance spectra of ATO films with different Ti content. The *inset* is the band-gap of ATO films as a function of the ratio of Ti and Al

Moreover, the smooth surface can help to achieve a high quality dielectric semiconductor interface for the devices. Thus, it is necessary to control the Ti concentration of ATO films in order to obtain high quality ATO films.

Figure 5 shows the transmittance of the ATO films on quartz substrates as a function of the Ti content in the wavelength range of 200–800 nm. The ATO films (with the Ti content less than 87 at%) are highly transparent in the visible range (400–700 nm) with the average transmittance of more than 85 %. The shift in the fundamental absorption edge towards shorter wavelengths is clearly observed when the Al amount in the films was increased. For determination of the optical band gap (Eg), the values of absorption coefficient α were in accord with Tauc's formula [21, 22]. The inset shows the direct optical band gap as a function of the ratio of Ti and Al. With the increasing of the Al content in the ATO films, the Eg increases from 3.6 eV

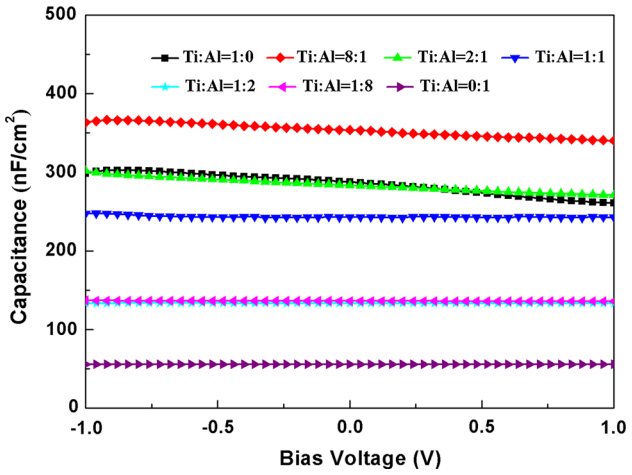

Fig. 6 Capacitance–voltage characteristics of ATO films measured at 100 kHz

(Ti:Al = 1:0) to 5 eV (Ti:Al = 1:8). Pure Al_2O_3 film has a band gap (8.9 eV) which is much more than 6 eV, thus couldn't use Tauc's formula in this situation.

Capacitance–voltage (C–V) measurement is an effective method to evaluate charge behaviors in the oxide films and at the interface, including mobile charges in the film, fixed charges, and interface-trapped charges [23]. The relative dielectric constants (ε_r) of the ATO film (100 nm) were examined from the MIM capacitance at 100 kHz. Figure 6 shows the capacitance–voltage characteristics of ATO films. It was found that as Ti content of ATO films exceeds 50 at%, the capacitance value had a little instable as bias voltage sweep from −1 to 1. This instability observed were originated from the spread of the charge carriers inside the insulator, which can caused by off-stoichiometry. Because Ti has several stable oxidation states of Ti^{3+} and Ti^{4+} which lead to a well known problem with materials containing Ti–O bonds: a reduced oxide. Such a reduced oxide has created many oxygen vacancies which act as carrier traps and increases the spread of the charge carriers inside the insulator [24]. Besides, the rough surface as well as R_{P-V} suddenly increasing (as shown in Fig. 4) and the mobile charges in the oxide and/or charge trapping into the oxide both aggravated the instability. According to the function as follow:

$$C = \frac{\varepsilon_o \varepsilon_r}{d} S \quad (1)$$

where ε_0 is the vacuum permittivity, ε_r represents the relative permittivity of ATO films, S is effective surface area of the dielectric film, and d denotes the thickness of the oxide film. Therefore the calculated ε_r of the ATO films with the ratio of Ti and Al (Ti:Al = 1:0, 8:1, 2:1, 1:1, 1:2, 1:8 and 0:1) are 32.7, 38.8, 33.5, 27.6, 16.5, 15 and 6.5, respectively. The relatively low dielectric constants of

solution-derived oxides with respect to the corresponding stoichiometric crystalline counterparts (e.g., $k(Al_2O_3) = 9$) are mainly due to the presence of small amounts of organic residues, slightly incomplete oxide lattice formation, and partial densification [25]. Most dopants showed the critical drawback in the high-k oxide that they caused decreased dielectric constants due to the intrinsically lower dielectric constant of the dopants than that of metal atom [26]. It is accordance with the HfO_2–Al_2O_3(HAO) films and ZrO_2–Al_2O_3(ZAO) films, which dielectric constant of HAO and ZAO are reduced to 10–20 due to the relatively low ε-value of Al_2O_3 [27]. Furthermore, according to the Lichtteneker's mixing rule [28], the dielectric constant of the ATO film increases evidently with the increasing of the Ti content, it is almost identical to our results. Meanwhile, the ε_r of ATO films with 13 at% Ti content is twice as much as that of pure Al_2O_3 film indicating that Ti addition can significantly improve the permittivity of Al_2O_3 film [29].

Current–voltage (I–V) measurements on the same devices were used to evaluate leakage current density and dielectric breakdown voltage. It is known that in thin film transistor (TFT) devices, the leakage current density of dielectric should be nearly 10^{-6} A/cm^2 at 1 MV/cm. As shown in Fig. 7, breakdown voltage of the ATO films was increases as Ti content decreases. Besides, leakage current for pure Al_2O_3 film was 3.41×10^{-8} A/cm^2 at 1 MV/cm, whereas when Ti content was increased from 13 to 50 at%, the leakage current values declined from 1.41×10^{-6} A/cm^2 at 1 MV/cm to 9.7×10^{-3} A/cm^2 at 1 MV/cm. The leakage current density of ATO films are obviously deteriorated with the content of Ti in the ATO films increases. Combined with the AFM results, high R_{P-V} may be one of critical factors leading to the extremely difference of leakage current and breakdown voltage, since a rough surface typically results in a high electric field, leading to exponentially increasing leakage current. Meanwhile, Yong et al. demonstrated that nanolaminated Al_2O_3–TiO_2 thin film with thicker Al_2O_3 interlayer has less leakage current densities, since insulating Al_2O_3 interlayer can prohibit leakage channels [13]. Therefore, the dielectric properties of ATO films are easily affected by the proportion of Al. As the concentration of Ti more than 50 at%, the ATO films exhibits sudden increase of leakage current under the electric field of 0.5 MV/cm, it can be seen that, TiO_2 is not an insulator but a large band gap semiconductor [30].

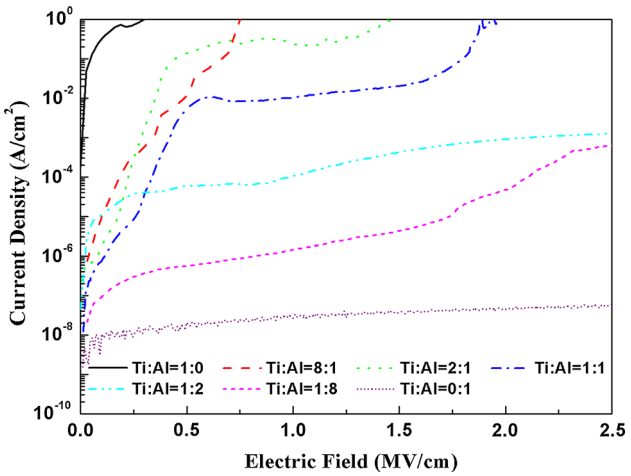

Fig. 7 Leakage current density of ATO films as a function of voltage bias

4 Conclusion

In summary, we have demonstrated the ATO films processing by using an organic–inorganic hybrid precursor solution. The effect of Ti concentration on the property of the ATO films was investigated. The ATO films were highly transparent in the visible range. At the annealing temperature of 400 °C, the ATO films were amorphous when Ti content in the ATO films is less than 67 at% and the ATO film was dense and free of pin hole. The RMS roughness, permittivity and leakage current density of TAO films were proportional to the Ti content, while the optical band gap showed an inverse correlation. The ATO films with 13 at% Ti concentration had the best performance, with the RMS roughness of 0.33 nm, R_{P-V} of 1.86 nm, relative permittivity of 15, and leakage current density of 1.41×10^{-6} A/cm^2 at 1 MV/cm. Herein, the ATO film with moderate Ti content is one of the promising dielectric materials for high-k gate dielectric applications.

Acknowledgments This work is supported by the National Natural Science Foundation of China under Grant 61006005, the Shanghai Science and Technology Commission under Grant 13520500200 and 14XD1401800, and the Shanghai Visiting Oriental Scholar Program.

References

1. Shi L, Xia YD, Xu B, Yin J, Liu ZG (2007) Thermal stability and electrical properties of titanium–aluminum oxide ultrathin films as high-k gate dielectric materials. J Appl Phys 101:034102
2. Meyers ST, Anderson JT, Hong D, Hung CM, Wager JF, Keszler DA (2007) Solution-processed aluminum oxide phosphate thin-film dielectrics. Chem Mater 19:4023–4029
3. Song K, Yang W, Jung Y, Jeong S, Moon J (2012) A solution-processed yttrium oxide gate insulator for high-performance all-solution-processed fully transparent thin film transistors. J Mater Chem 22:21265–21271
4. Choi S, Park BY, Jang M, Jeong S, Lee JY, Ryu BH, Seong TY, Jung HK (2011) Solution processed high-k lanthanide oxides for low voltage driven transparent oxide semiconductor thin film transistors. ECS Trans 35(4):901–908

5. Li XF, Xin EL, Zhang JH (2013) Low-temperature solution-processed zirconium oxide gate insulators for thin-film transistors. IEEE T Electron Dev 60(10):3413–3416
6. Yoo YB, Park JH, Lee KH, Lee HW, Song KM, Lee SJ, Baik HK (2013) Solution-processed high-k HfO_2 gate dielectric processed under softening temperature of polymer substrates. J Mater Chem C 1:1651–1658
7. Novkovski N, Paskaleva A, Atanassova E (2005) Dielectric properties of rf sputtered Ta_2O_5 on rapid thermally nitrided Si. Semicond Sci Technol 20:233–238
8. Kim KM, Kim CW, Heo JS, Na H, Lee JE, Park CB, Bae JU, Kim C-D, Jun M, Hwang YK, Meyers ST, Grenville A, Keszler DA (2011) Competitive device performance of low-temperature and all-solution processed metal-oxide thin-film transistors. Appl Phys Lett 99:242109
9. Avis C, Jang J (2011) High-performance solution processed oxide TFT with aluminum oxide gate dielectric fabricated by a sol–gel method. J Mater Chem 21:10649–10652
10. Pu HF, Li HL, Yang Z, Zhou QF, Dong CY, Zhang Q (2013) Effect of content ratio on solution-processed high-k titanium–aluminum oxide dielectric films. ECS Solid State Lett 2(10):N35–N38
11. Adamopoulos G, Thomas S, Bradley DDC, McLachlan MA, Anthopoulos TD (2011) Low-voltage ZnO thin-film transistors based on Y_2O_3 and Al_2O_3 high-k dielectrics deposited by spray pyrolysis in air. Appl Phys Lett 98:123503
12. Fröhlich K, Ťapajna M, Rosová A, Dobročka E, Hušeková K, Aarik J, Aidla A (2008) Growth of high-dielectric-constant TiO_2 films in capacitors with RuO_2 electrodes. Electrochem Solid-State Lett 11(6):G19–G21
13. Kim YS, Yun SJ (2005) Nanolaminated Al_2O_3–TiO_2 thin films grown by atomic layer deposition. J Cryst Growth 274:3–4
14. Song XM, Takoudis CG (2007) Cyclic chemical-vapor-deposited TiO_2/Al_2O_3 film using trimethyl aluminum, tetrakis(diethylamino)titanium, and O_2. J Electrochem Soc 154(8):G177–G182
15. Lim JW, Yun SJ, Kim HT (2007) Characteristics of $Al_xTi_{1-x}O_y$ films grown by plasma-enhanced atomic layer deposition. J Electrochem Soc 154(11):G239–G243
16. Auciello O, Fan W, Kabius B, Saha S, Carlisle JA, Chang RPH, Lopez C, Irene EA, Baragiola RA (2005) Hybrid titanium–aluminum oxide layer as alternative high-k gate dielectric for the next generation of complementary metal–oxide–semiconductor devices. Appl Phys Lett 86:042904
17. Rowlette PC, Wolden CA (2010) Pulsed plasma-enhanced chemical vapor deposition of Al_2O_3–TiO_2 nanolaminates. Thin Solid Films 518:3337–3341
18. Liu JH, Guo Q, Yu M, Li SM, Yao L (2013) Formation and dielectric properties of Al–Ti–O nanocomposite oxide film on aluminum using sol–gel and anodizing. ECS J Solid State Sci Technol 2(3):N55–N60
19. Almeida RM, Christensen EE (1997) Crystallization behavior of SiO_2–TiO_2 sol–gel thin films. J Sol-Gel Sci Technol 8:409–413
20. Zhao YP, Wang GC, Lu TM (1999) Surface-roughness effect on capacitance and leakage current of an insulating film. Phys Rev B 60(12):9157–9164
21. Tauc J, Grigorovici R, Vancu A (1966) Optical properties and electronic structure of Ge. Phys Status Sol 15:627–637
22. Vitanov P, Babeva T, Alexieva Z, Harizanova A, Nenova Z (2004) Optical properties of $(Al_2O_3)_x(TiO_2)_{1-x}$ films deposited by the sol–gel method. Vacuum 76:219–222
23. Dhananjay, Krupanidhi SB (2007) Low threshold voltage ZnO thin film transistor with a Zn0.7Mg0.3O gate dielectric for transparent electronics. J Appl Phys 101:123717
24. Wilk GD, Wallace RM, Anthony J (2001) High-K gate dielectrics: current status and materials properties considerations. J Appl Phys 89(10):5243–5275
25. Yang W, Song K, Jung Y, Jeong S, Moon J (2013) Solution-deposited Zr-doped AlOx gate dielectrics enabling high-performance flexible transparent thin film transistors. J Mater Chem C 1(27):4275–4282
26. Ko J, Kim J, Park SY, Lee E, Kim K, Lim KH, Kim YS (2014) Solution-processed amorphous hafnium–lanthanum oxide gate insulator for oxide thin-film transistors. J Mater Chem C 2(6):1050–1056
27. Aoki Y, Kunitake T (2004) Solution-based fabrication of high-*k* gate dielectrics for next-generation metal-oxide semiconductor transistors. Adv Mater 16(2):118–123
28. Lee WH, Wang CC, Chen WT, Ho JC (2008) Characteristic of organic thin film transistor with a high-k insulator of nano-TiO2 and polyimide blend. Jpn J Appl Phys 47(12R):8955–8960
29. Vitanov P, Harizanova A, Ivanova T, Ivanova K (2003) Deposition and dielectric properties of $(Al_2O_3)_x(TiO_2)_{1-x}$ thin films. J Mater Sci: Mater Electron 14:757–758
30. Robertson J, Xiong K, Clark SJ (2006) Band structure of functional oxides by screened exchange and the weighted density approximation. Phys Stat Sol (B) 243(9):2054–2070